

International Conference on Space Optics—ICSO 2008

Toulouse, France

14–17 October 2008

Edited by Josiane Costeraste, Errico Armandillo, and Nikos Karafolas



Dynamic diffraction gratings and a spectrometer demonstrator

Ville-Veikko Aallos

Rami Mannila

Heikki Saari

Kai Viherkanto

et al.



DYNAMIC DIFFRACTION GRATINGS AND A SPECTROMETER DEMONSTRATOR

Ville-Veikko Aallos⁽¹⁾, Rami Mannila⁽¹⁾, Heikki Saari⁽¹⁾, Kai Viherkanto⁽¹⁾, Luis Venancio⁽²⁾

⁽¹⁾VTT, P.O. Box 1000, FI-02044, Finland, Ville-Veikko.Aallos@vtt.fi

⁽²⁾European Space Agency, 2200 AG Noordwijk, The Netherlands, Luis.Miguel.Gaspar.Venancio@esa.int

ABSTRACT

This paper describes the outcome of the ESA contract 20532/06/NL/Sfe entitled “Instrument concepts using dynamic diffraction gratings”. The goal of the project was to study the optical performance of state of the art dynamic diffraction grating technology and identify potential applications for space missions. A dynamic diffraction grating sample was obtained for characterisation and a demonstrator for a compact spectrometer architecture was implemented and tested.

1. INTRODUCTION

Dynamic diffraction gratings are gratings where some of their optical or geometrical properties can be actively controlled in order to provide phase shifts to an incoming light beam. Here the scope is restricted to reflection gratings fabricated by MEMS processes and such a component is called a PMDG (programmable micro diffraction grating).

2. PROGRAMMABLE MICRO DIFFRACTION GRATINGS

Commercially successful PMDG components include the Grating Light Valve [1] and the Polychromator [2]. Other PMDG designs are described in papers about the MEMS compound grating (MCG) [3], grating electromechanical system (GEMS) [4], grating light modulator (GLM) [5], piezoelectric tunable grating [6] and the pitch tunable variable blaze grating [7]. In terms of technology readiness for space applications, the Polychromator has the highest maturity as a spectrometer based on this PMDG technology will fly on the NASA LCROSS mission. The Polychromator consists of a linear array of reflecting elements. The width of the elements is typically $1..10 \times \lambda$ in order to obtain large enough diffraction angles. The length of the elements is restricted by manufacturing considerations and surface flatness tolerances. Lengths of up to 10 mm have been demonstrated. The elements are displaced by electrostatic actuation. Depending on the required phase shift for the application the maximum displacement is either $\lambda/4$ or $\lambda/2$. The elements can be controlled either individually or grouped in pixels (with 6 to 10 elements), where every second element is static and

every second element of the pixel moves in concert. PMDGs with up to 6000 elements (1000 pixels) [1] or 1000 individually controlled elements have been demonstrated [8]. The control electronics is a significant part of the whole PMDG system.

3. PMDG FUNCTIONS

PMDGs can be used for programmable angular dispersion or for spatiotemporal light modulation.

There are PMDG designs where the grating pitch can be continuously changed up to 10 % [7]. With the discrete element PMDG design programmable rectangular or triangular grating profiles could be created. With such a component switchable configurations could be made to conventional grating spectrometers. Simulations for a reconfigurable binary grating is shown in Fig. 1 and for a staircase variable blaze grating in Fig. 2.

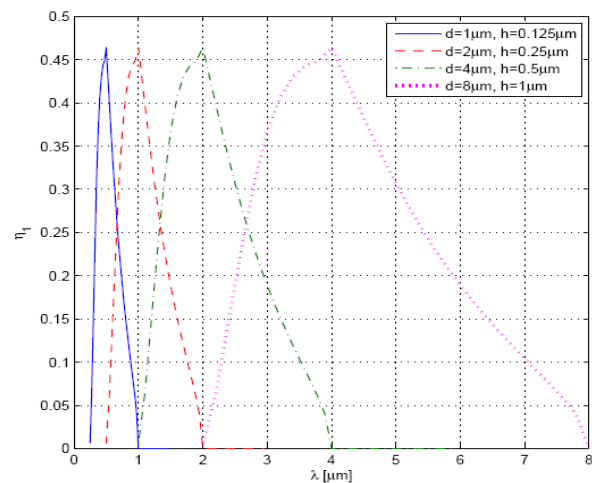


Fig. 1. Simulation of diffraction efficiency η_1 for a hypothetical reconfigurable PMDG consisting of $0.5 \mu\text{m}$ wide elements with different periods d and depths h .

The groove depths are chosen to optimize the first order diffraction efficiencies of wavelengths $d/2$. It follows from the grating equation that as the ratio between the period and the wavelength remains same, all central wavelengths of the shown bands are diffracted into the same angle. This means that the detector position can remain fixed when different spectral areas are chosen by changing the grating parameters. Moreover, since the

angular dispersion decreases with the increasing period, the wider bands obtained for longer wavelengths will fit approximately into the same detector area.

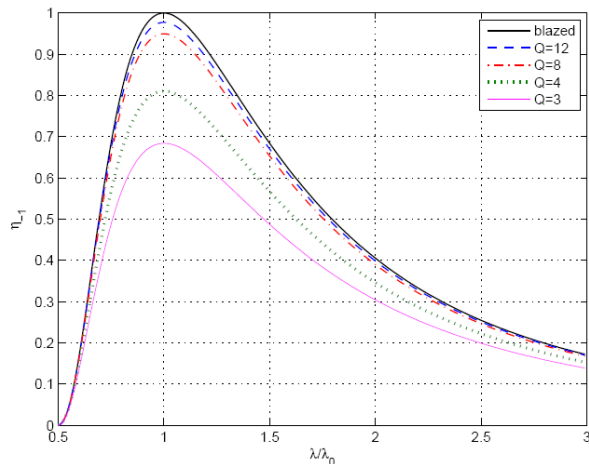


Fig. 2. Diffraction efficiencies of the order $m=-1$ for a staircase PMDG approximating the ideal blazed profile with Q levels and an ideal blazed profile.

The more useful function has so far been spatiotemporal light modulation with numerous applications in video projectors, printing systems and spectrometers. Considering space applications the spectrometer applications are relevant. There are two different approaches. When a collimated broadband beam of light is used the PMDG can be used as a diffractive filter performing a programmable spectral modulation. The same end result is obtained by using a dispersed focused beam on the PMDG. With this function correlation spectrometers [8] and Hadamard transform spectrometers [2] can be implemented.

Compared with other spatial light modulators (SLM) such as liquid crystal displays (LCD) and micro mirror arrays, PMDGs can operate in the IR domain, have a fast response and provide direct analogous control of the modulation. A drawback of the PMDGs is the dispersion caused by the grating structure, which restricts the cone angles of the incoming beam and produces straylight in higher diffraction orders.

4. CHARACTERISATION OF A PMDG SAMPLE

PMDGs are not yet easily available as standalone components. Therefore, at the time of this project, the only way to obtain a PMDG sample was to procure a DTS-1700 spectrometer from Polychromix and remove its PMDG along with the control electronics. This PMDG has an active area of ca 12x2 mm consisting of 1000 elements (Fig. 3). The electrical connections to the elements are organised so that 100 pixels consisting of 10 elements are formed, where every second element is static and every second element can be pulled down

with a voltage of 15..30 V controlled with 8-bit resolution.



Fig. 3. Photo of the PMDG sample within its package.

The modulation performance of the PMDG was investigated with green and red HeNe laser beams (543.3 nm and 632.8 nm). The beam (0.5 mm spot size) was directed with a 0° angle of incidence and the diffracted signals were observed on a screen with a CCD camera. The measured signal intensities for the range of control voltages is shown in Fig. 4.

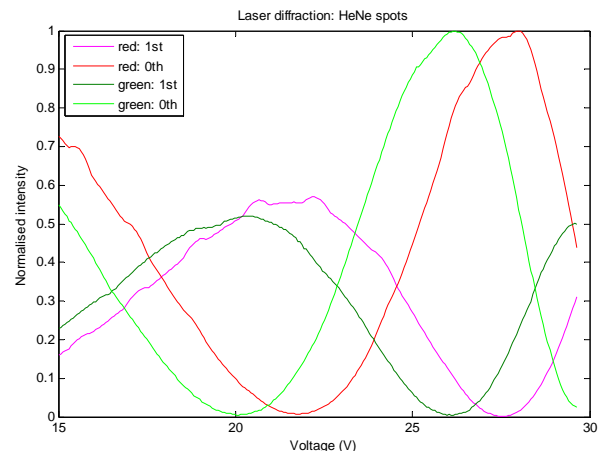


Fig. 4. Relative intensity of the 0^{th} order (reflected) and 1^{st} order spots versus control voltage.

The initial deflection (with the 15 V bias voltage on) and total deflection can be estimated to be about 80 nm and 375 nm based on the phases of the intensity curves. The obtainable contrast ratio between the 0^{th} or 1^{st} order maximum or minimum signal is at least 500.

From electrostatic theory, the following model (Eq. 1) can be fitted to the deflection versus control voltage [1].

$$\delta(V) = \frac{x_0}{3} \left[1 - \left(1 - \left(\frac{V}{V_{PI}} \right)^\omega \right)^{\frac{2}{3\omega}} \right], \quad (1)$$

where V_{PI} is the pull-in voltage, x_0 is the original gap, and ω is a fitting parameter. The fitting parameter used here is the same as in the original GLV model, $\omega = 1.8$. Other parameters are $x_0 = 2180$ nm and $V_{PI} = 32.2$ V.

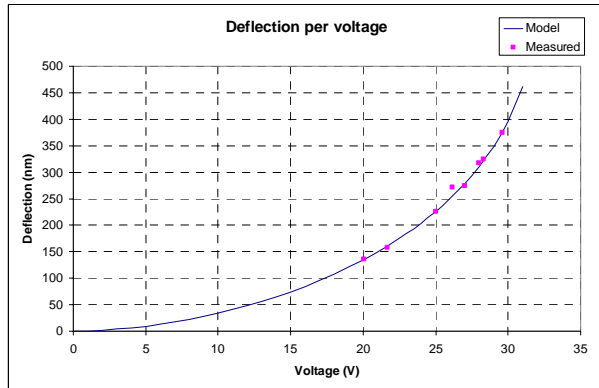


Fig. 5. Results of the model of deflection versus control voltage for the PMDG sample. In addition to the HeNe points, measurements were obtained from longer wavelengths.

It can be seen that most of the deflection occurs in the latter half of the control voltage range and it makes sense to use a bias voltage and a smaller range of controllable voltage.

When the spot size is reduced to 90 μm with a microscope objective and scanned along the PMDG elements with deflection set to $\lambda/4$, the intensity profile shown in Fig. 6 is obtained.

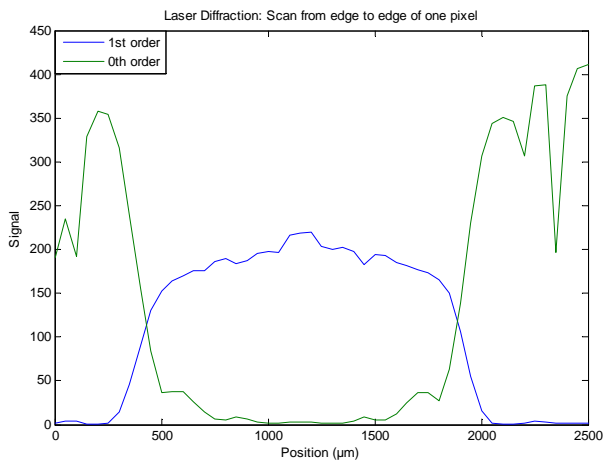


Fig. 6. The diffraction spot intensity from a scan along one pixel in diffractive state with 50 μm steps. The signal in the 0th order is from outside the pixel structure

The deflection along the pixel length has some variation and the usable length is ca 1.2 mm of the full 2 mm.

The diffraction efficiency of the PMDG sample referred to a reference gold mirror was measured by moving a silicon detector on a swing arm centered on the PMDG. The resulting reflection and diffraction directions are shown in Fig. 7.

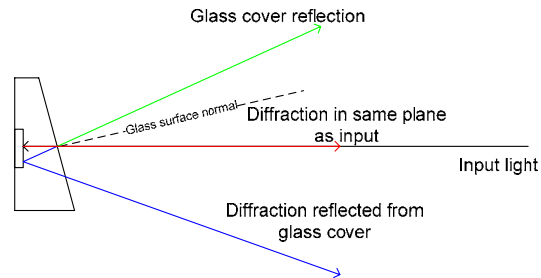


Fig. 7. Illustration of the light paths from the PMDG sample in the diffraction efficiency measurement.

A reflection coefficient of 0.95 was assumed for the gold mirror. Only points where $>0.1\%$ of incoming light is going, are noted separately in Table 1. The values in even diffraction orders for reflection are caused by the gaps in the grating structure. They are actually the 1st, 2nd etc orders for the non-actuated grating but as they are the same points as even orders for actuated grating, it is clearer to present them this way.

Table 1. Distribution of incoming light intensity to different orders for a 632.8 nm HeNe laser with the PMDG sample set to reflection or maximum diffraction.

| | Reflection | Diffraction |
|--|------------|-------------|
| Glass reflection | 4.75 % | 4.75 % |
| 0 order | 60.57 % | 0.72 % |
| 1 st order | 0.61 % | 64.96 % |
| 2 nd order | 4.73 % | <0.2 % |
| 3 rd order | <0.1 % | 7.07 % |
| 4 th order | 3.31 % | <0.1 % |
| 5 th order | <0.1 % | 1.54 % |
| 6 th order | 2.28 % | <0.1 % |
| 7 th order | <0.1 % | 0.82 % |
| 8 th order | 3.04 % | <0.1 % |
| 9 th order | <0.1 % | 0.44 % |
| Reflected refl/diff (0 th + 1 st) | 1.96 % | 1.87 % |
| Higher orders + absorption | 18.36 % | 17.43 % |

It is noteworthy that the even orders are suppressed in the diffractive state, which can also be seen with the following qualitative numerical model in Fig. 8.

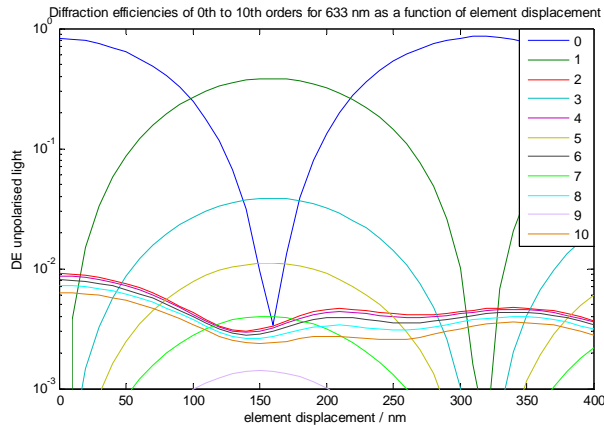


Fig. 8. Simulated diffraction behaviour for ten first orders for 633 nm. All the even orders are suppressed when the grating is in diffractive state but they do have a maximum with zero order when the displacement is 0 nm.

5. INSTRUMENT CONCEPTS FOR THE PMDG SAMPLE

The PMDG sample characterised is already successfully used in the Polychromix Hadamard transform spectrometer to modulate a spectrum dispersed by a grating [2].

Two instrument concepts were envisaged for this PMDG sample. The first is an imaging correlation spectrometer shown in Fig. 9 for the near infrared domain.

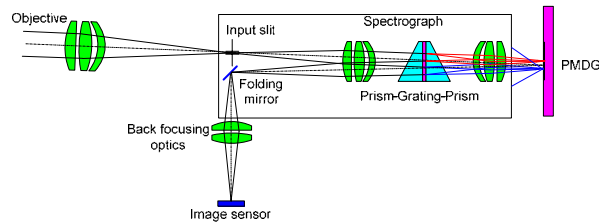


Fig. 9. An instrument concept for an imaging programmable spectrometer. An off-axis concept with one spectrograph and a PMDG. The wavelengths marked with red are selected and thus reflected back through the spectrograph to the sensor, but the wavelengths marked with blue are diffracted and are not detected by the image sensor.

The spectral angle mapper (SAM) algorithm used in hyperspectral data processing can be approximated with this concept by taking two consecutive images or having two parallel channels. The first with a searched spectral signature programmed on the PMDG and the second with no signature. The ratio of these images is proportional to the correlation with the signature. An

implementation of this concept with a liquid crystal display SLM is described in [9] and with the GEMS in [10]. The smallest diffraction angle is 2.2° at $\lambda = 900$ nm for the PMDG sample. The marginal angle of the system must be limited to half of that so that the light that diffracts to angle of 2.2° and has the opening angle defined by the f-number does not overlap with the acceptance angle of the system. This turns out as f-number $f/\# = 26$, which exceeds the spectrograph $f/\# = 4$. Also the achievable field of view is limited with the <2 mm usable area on the PMDG in the spatial direction. Therefore the concept was not feasible with this PMDG sample. However a PMDG would be an ideal SLM for this concept as modulation capability is not required in the spatial direction and a PMDG can operate in the infrared domain.

The other concept is a small single-point spectrometer presented in Fig. 10. The fore optics focuses the light to a pinhole through a beam splitter which guides part of the incoming light to a monitoring detector. The light that goes through the pinhole is collimated and guided through a linear variable bandpass filter (LVBF) that passes different spectral bands on different parts of the filter thus separating the spectral bands. The PMDG does a Hadamard transform [11] or line scan through the spectrum and the reflected light returns to the pinhole. The diffracted light does not hit the pinhole because of its slightly different incident angle on the collimator. A beam splitter guides the reflected light through a focusing lens to a single detector element. This concept can also operate in a correlation spectrometer mode. Using the LVBF for waveband separation makes possible a compact design, but has the drawback of reducing the throughput.

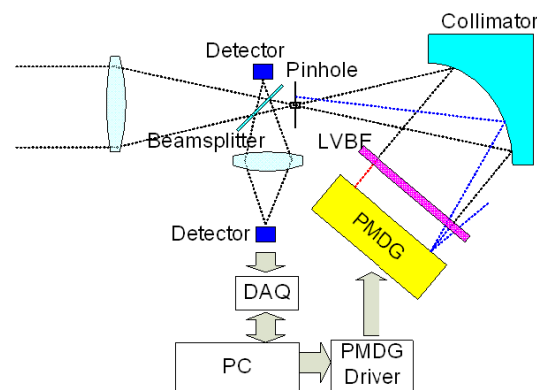


Fig. 10. A single-point miniature spectrometer. An on-axis concept with beam splitter, LVBF and PMDG.

Implementation of a demonstrator for the miniature spectrometer was feasible with this PMDG sample.

6. SPECTROMETER DEMONSTRATOR DESIGN

Specifications for the miniature spectrometer demonstrator are shown in Table 2.

Table 2. Specifications for the demonstrator.

| Description | Value | Rationale |
|---------------------|--------------|---|
| Wavelength range | 620-1080 nm | Readily available LVBFs from JDSU. |
| Spectral resolution | 1-2 % of CWL | Bandwidth of the LVBFs |
| Throughput | max 0.07 % | The efficiency of the LVBF for "dispersion" is inherently its relative bandwidth (~0.01). |

The optical design of the demonstrator is presented in Fig. 11.

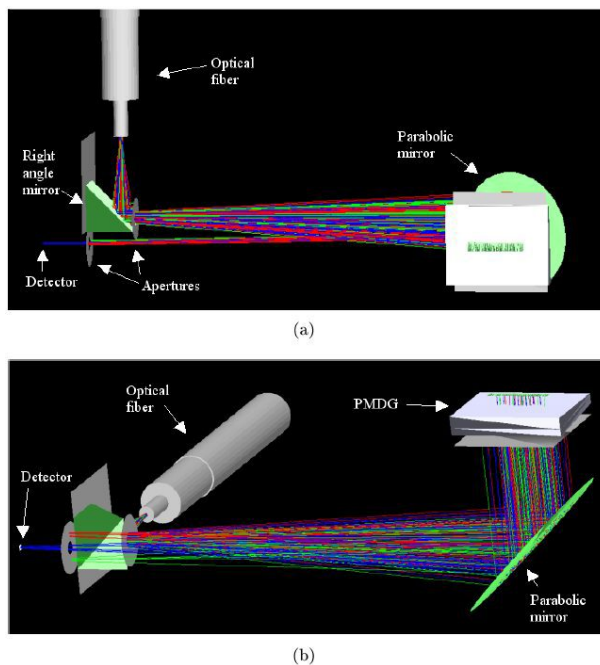


Fig. 11. Demonstrator optical design. (a) Side view. (b) Bottom view. Blue rays are accepted rays and green and red rays are rejected rays.

Light enters the system from a 600 μm optical fibre or from a lens assembly and 600 μm pinhole. The input light beam is then directed with a right angle mirror to an off-axis parabolic mirror which collimates the beam. The right angle mirror was added to the system to make more space for mechanical attachment of the fibre and the detector. There is an aperture in front of the PMDG to block light from hitting the surface around the PMDG active area which would cause unwanted reflection. The LVBF is mounted on the backside of this aperture, which is tilted 1° in order to avoid ghost reflections from the LVBF and the aperture itself. If the tilting angle of the LVBF were significantly larger it would

affect transmission through the LVBF, and if it were smaller, ghost rays would not be separated from accepted rays in the detector plane. The tilting is done in the shorter dimension of the LVBF so that the incoming light and the light reflected from the PMDG will go through the same pass band. The cover glass of the PMDG package is tilted ca 5.5° and thus it does not cause ghost reflection. For the accepted light rays the PMDG is a mirror surface and for the rejected rays a common diffraction angle based on the smallest diffracted angle is used. There are two other apertures in the system, one after the right angle mirror limiting the input beam half cone angle and another in front of the detector allowing only wanted rays to hit the detector. Rejected rays do not hit the exit aperture because their light path is different by a few degrees.

If the LVBF would be directly integrated on the PMDG the optical system volume of this spectrometer would be very compact. However, in the demonstrator implementation (Fig. 12), volume was not optimised and a focal length of 102 mm was selected to be compatible with visual domain LVBFs also. For the NIR domain a focal length of 50 mm would be enough.

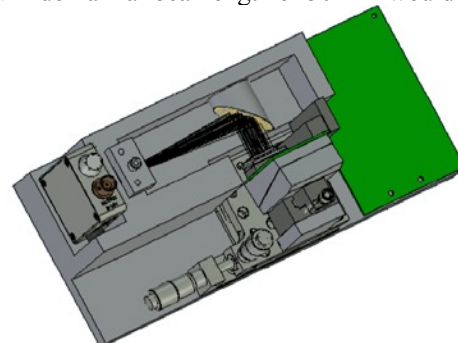


Fig. 12. Demonstrator opto-mechanical design. The PMDG sample is mounted on a tilt and translation platform.

The demonstrator components are shown in Table 3.

Table 3. Demonstrator components.

| Component | Description |
|-----------------------|--|
| Parabolic mirror | Effective focal length = 101.6 mm, gold coated off-axis mirror |
| LVBF | 620 – 1080 nm, BW = 1.5%, transmission 90 % at 900 nm 1400 – 1700 nm, BW = 0.6%, transmission 45% at 1400 nm |
| PMDG | Sample disassembled from Polychromix DTS-1700 spectrometer. Active area 2x12 mm, 100 pixels of 120x2000 μm size |
| Right angle mirror | Gold coated, size of the reflecting surface is 10x14.1 mm |
| VIS-NIR or NIR sensor | Si and InGaAs detectors with 0.8 mm ² active area |

7. DEMONSTRATOR TEST RESULTS

The results described here were measured with the visual domain configuration.

Centre wavelengths were defined with a reference Ocean Optics HR4000 spectrometer in place of the detector. The measurements were carried out by programming a pattern with every fourth pixel in diffracting state and making four measurements to get all the pixels in diffracting state. The centre wavelengths were then checked from the modulated spectra by defining the centre point of each modulated signal minima. Using these centre wavelengths the control voltages were then calculated from the model. The control voltages were also measured and there is some variation between measured values and values from the model. There is also some variation between individual pixels on some wavelength range meaning that some pixels require higher or lower voltages than neighbouring pixels in general. The model is of course unaware of such features.

Neighbouring pixels have an effect on the contrast ratio. This is clearly visible between one and two pixels. Adding a third pixel does not add much to the contrast but will keep the centre wavelength the same (see Fig. 13). The FWHM bandwidth of the LVBF is 1.5% which means 10.5 nm @ 700 nm. The dispersion is almost constant at about 40 nm/mm which turns out as about 4.8 nm shift in wavelength per pixel (120 μ m). So the spectral bandwidth for each pixel is wider than the spectral shift between adjacent pixels and thus the bands will overlap. This will increase spectral resolution but may have an effect to the relative spectral features. What is actually measured is the difference in signal between reflected and diffracted states. If the modulation is not clear enough, some spectral features will remain unnoticed.

The demonstrator input fibre was illuminated with FWHM = 4 nm monochromator lines and the signal was measured with line scan and Hadamard methods. The signal levels were rather low and because the measurement time is 2 minutes (about 1 s per measurement point or pattern from which 50 ms is for signal integration and rest is for pattern change due to the software implementation), the detector or amplifier can be seen drifting slowly throughout the measurements. The drifting is in a scale of μ V but it has an effect with these signal levels. For line scan this means that the bottom line is not horizontal. The Hadamard scan handles small drifts in a cleaner way and the drifting causes only some signal spikes, negative or positive depending on the drift, on certain locations of the spectrum that are directly related to the size of the Hadamard matrix.

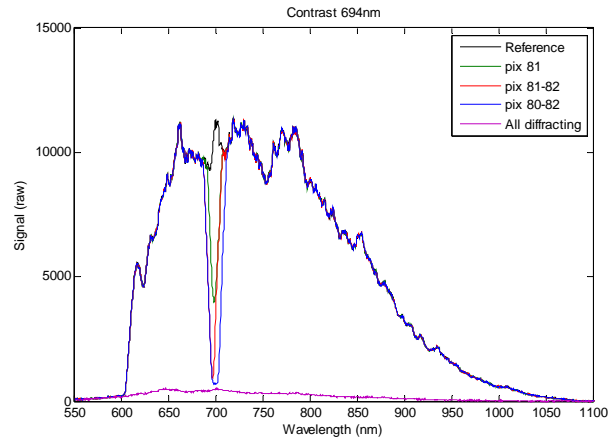


Fig. 13. Demonstrator modulation contrast with one, two and three pixels in diffracting state. The background signal in the all in a diffractive state is due to diffuse ghost reflection from the LVBF aperture.

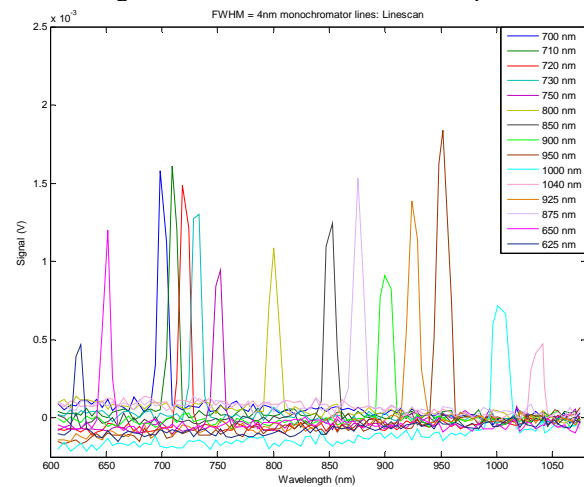


Fig. 14. Monochromator lines measured with the line scan method.

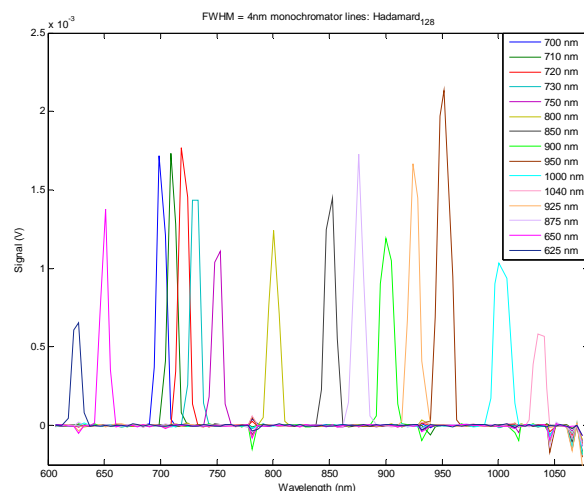


Fig. 15. Monochromator lines from HR640 measured with Hadamard method. The small spikes where multiple lines can be seen are caused by the drift.

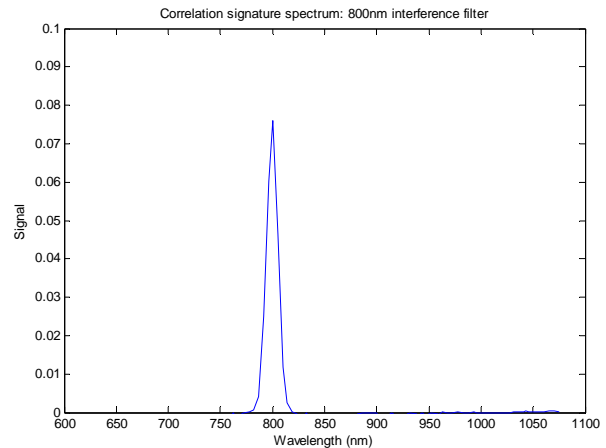
The SNR improvement factor with Hadamard scan can be calculated from the noise levels to be 6.5. Theory gives a value of 5.6. The difference is due to the small drift in the line scan measurement. When corrected, the improvement factor is about 5.0.

As a result from these measurements for the demonstrator in the visual configuration, the spectral range can be determined to be 609-1060 nm, spectral resolution is <1.5 % of centre wavelength and absolute wavelength accuracy is ± 1.0 nm for most of the wavelength range. The measured maximum throughput is <0.2 % which restricts the possible applications for this spectrometer.

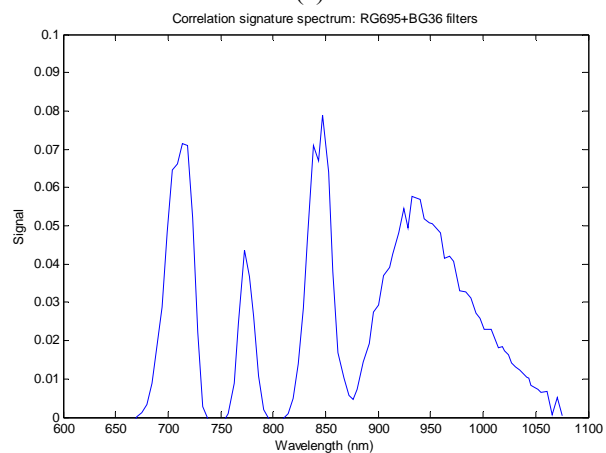
Correlation mode measurements were done with a few filter transmissions. A signature was made of a 800 nm interference filter and was tested against various other filters. Another signature was made of RG695 and BG36 filters and was again tested against various other filters (Fig. 16). The signature means that the PMDG is programmed to reflect signal according to the measured transmission spectra. The measurement takes two signal values, one with the signature and the other with a fully reflecting grating. The signature signal is then divided with the reflected signal. The values shown in Table 4 are obtained. Correlation results are in line with what was to be expected with this approximation of the SAM method.

Table 4. Correlation results of different filter spectra with signatures from 800 nm interference filter (BP800) and RG695+BG36 filters (- means untested).

| Test signal from | BP800 Correlation | RG695+BG36 Correlation |
|------------------|----------------------|---------------------------|
| BP700 | 0.29 | - |
| BP766 | 0.25 | 0.49 |
| BP800 | 0.77 | 0.22 |
| BP830 | 0.22 | - |
| BP880 | 0.23 | - |
| BP905 | 0.29 | - |
| BP940 | 0.31 | - |
| RG850 | 0.09 | 0.48 |
| RG695 | 0.14 | 0.40 |
| raw halogen | 0.15 | 0.40 |
| RG695+BG36 | - | 0.60 |
| BG36 | - | 0.53 |



(a)



(b)

Fig. 16. Sample spectra for correlation signatures were taken from halogen lamp through a) 800 nm interference filter and b) RG695+BG36 filters. The signature means that the PMDG is programmed to reflect signal according to the measured transmission spectra.

8. CONCLUSIONS

PMDGs are attractive components for spatial light modulation in the infrared domain. Hadamard transform, correlation, reconfigurable spectrometers and laser pulse shaping applications are being investigated.

The structure of a PMDG is rather simple and robust and therefore no unsurmountable obstacles are expected for space qualification. Special attention must be paid to electrostatic protection.

The presented instrument demonstrator concept has a quite compact optical volume, but the throughput is rather low even for optimised components. The concept provides an alternative to LVBF spectrometers with detector arrays. Operation of the PMDG requires an electrostatic control system and this must be traded against having similar electronic complexity in an LVBF spectrometer based on a linear array detector.

9. REFERENCES

1. Jahja I. Trisnadi, Clinton B. Carlisle and Robert Monteverde, Overview and applications of Grating Light Valve™ based optical write engines for high-speed digital imaging, Photonics West 2004 – Micromachining and Microfabrication Symposium, January 26, 2004, San Jose, CA, USA
2. Stephen D. Senturia, David R. Day, Michael A. Butler and Malcolm C. Smith, Programmable diffraction gratings and their uses in displays, spectroscopy and communications, *J. Microlith., Microfab., Microsyst.* 4(4), Oct–Dec 2005
3. Jaap Verheggen, Ganesh Panaman and James Castracane, Characterization and fabrication of MOEMS-based optical switching elements, MOEMS Display, Imaging, and Miniaturized Microsystems IV, Proceedings of SPIE Vol. 6114
4. Marck W. Kovarz, John C. Brazas, Jr. and James G. Phalen, Conformal grating electromechanical system (GEMS) for high-speed digital light modulation, IEEE, 15th Int. MEMS Conf. Digest, 568-573, 2002
5. Zhihai Zhang, Shanglian Huang, Yi Wu, Xu Yan, Jie Zhang and Hongqiao Fu, Fabrication improvement of the grating light modulator, Proceedings of the 1st IEEE International Conference on Nano/Micro Engineered and Molecular Systems, January 18 - 21, 2006, Zhuhai, China
6. Chee Wei Wong, Yongbae Jeon, George Barbastathis and Sang-Gook Kim, Analog piezoelectric-driven tunable gratings with nanometer resolution, *Journal of Microelectromechanical Systems*, Vol. 13, No. 6, December 2004
7. Yu-Sheng Yang and Cheng-Hsien Liu, Design and fabrication of a pitch tunable blaze grating, MEMS/MOEMS Components and Their Applications II, Proceedings of SPIE Vol. 5717 (SPIE, Bellingham, WA, 2004)
8. Michael B. Sinclair, Kent B. Pfeifer, Michael A. Butler, Stephen D. Senturia, Erik R. Deutsch, Dan Youngner, Eugen Cabuz and G. Benjamin Hocker, A MEMS based correlation radiometer, MOEMS and Miniaturized Systems IV, Proceedings of SPIE Vol. 5346 (SPIE, Bellingham, WA, 2004)
9. Uula Kantojärvi, Kai Vihekanto, Ville Aallos, Heikki Saari, Esko Herrala and Bernd Harnisch, Performance of the imaging spectral signature instrument (ISSI) breadboard, Sensors, Systems, and Next-Generation Satellites XI, Proc. of SPIE Vol. 6744.
10. J. Daniel Newman, Marek W. Kowarz, James G. Phalen, Paul P. K. Lee and A. D. Cropper, MEMS Programmable Spectral Imaging System for Remote Sensing, Spaceborne Sensors III, Proc. of SPIE Vol. 6220.
11. B.K. Harms, R.A. Dyer, S.A. Dyer, T.W. Johnson, and J.B. Park, An introduction to Hadamard spectrometry and the multiplex advantage, IEEE Instrumentation and measurement technology conference, IMTC-89 Conference Record, 6th IEEE, April 1989.